Quantum Chernoff bound metric for the *XY* model at finite temperature

Damian F. Abasto,[1,*] N. Tobias Jacobson,[1,†] and Paolo Zanardi[1,2]
[1]*Department of Physics and Astronomy, University of Southern California, Los Angeles, California 90089-0484, USA*
[2]*Institute for Scientific Interchange, Viale Settimio Severo 65, I-10133 Torino, Italy*
(Received 15 November 2007; published 28 February 2008)

We explore the finite-temperature phase diagram of the anisotropic *XY* spin chain using the quantum Chernoff bound metric on thermal states. The analysis of the metric elements allows one to easily identify, in terms of different scaling with temperature, quasiclassical and quantum-critical regions. These results extend recent ones obtained using the Bures metric and show that different information-theoretic notions of distance can carry the same sophisticated information about the phase diagram of an interacting many-body system featuring quantum-critical points.

DOI: 10.1103/PhysRevA.77.022327 PACS number(s): 03.67.−a, 03.65.Ud, 64.70.Tg, 24.10.Cn

I. INTRODUCTION

Quantum phase transitions (QPTs) are characterized by a dramatic change in the ground state of a many-body system prompted by a change of the parameters $\{\lambda\}$ specifying the Hamiltonian $H(\{\lambda\})$ of the system. Unlike classical phase transitions, which are driven by thermal fluctuations, quantum phase transitions occur at $T=0$ and are driven solely by quantum fluctuations. In particular, second order quantum phase transitions are characterized by a gap between the ground state and first excited state that vanishes at criticality [1].

The analysis of these transitions has benefited from tools of quantum information theory. The von Neumann entropy and fidelity applied to many-body systems can identify phase transitions and reveal different scaling behaviors at different regions of the phase diagram [2–7]. More recently it has been shown that the quantum fidelity—a distinguishability measure between quantum states—can identify the quantum phase transition by comparing two ground states corresponding to slightly different values of the coupling constants $\{\lambda\}$ [8–22]. This new approach provides an alternative to the study of phase transitions using order parameters and symmetry breaking patterns, which depends on *a priori* knowledge of the physics of the problem [23].

Another distinguishability measure for density operators was very recently introduced: the quantum Chernoff bound [24,25]. Suppose there are n copies each of two density matrices ρ and σ, i.e., $\rho^{\otimes n}$ and $\sigma^{\otimes n}$, and one set has been given to us. We know what ρ and σ are, but we do not know which set we received. There is always a two-outcome positive operator-valued measure (POVM) $\{E_0, E_1\}$ that measures and distinguishes one set of n-copy states from the other such that the probability of making a misidentification P_e is minimized. In general, this probability will depend on the number of copies. In the asymptotic limit of n very large, the probability of misidentification has a particularly simple exponential dependence on n given by $P_{e,\min}=e^{-n\xi_{QCB}}$. The quantity ξ_{QCB} is called the quantum Chernoff bound. It is a function of the density matrices only, with $\xi_{QCB}=-\ln[\min_{0\le s\le 1}\mathrm{Tr}(\rho^s\sigma^{1-s})]$. The classical version of this problem was analyzed for the first time by Chernoff [26]. It took 50 years to prove the quantum version of this problem.

The quantum Chernoff bound has many interesting properties. Among these is monotonicity under completely positive (CP) maps, which makes it a valid distinguishability measure [24]. In addition, ξ_{QCB} has an operational meaning arising from a statistical inference problem. Intuitively, we see that for a fixed probability of error P_e, the larger ξ_{QCB} is the smaller the number of copies of ρ and σ we will need in order to distinguish them.

In the present work, we apply the quantum Chernoff bound as a distinguishability measure to the manifold of Gibbs or thermal states associated with the anisotropic *XY* model in a transverse magnetic field. In the spirit of the information-theoretic and differential geometric approach advocated in [10], we will compare states corresponding to Hamiltonians with slightly different values of the parameters $\{\lambda\}$ to derive a metric tensor for the parameter manifold itself. This metric detects the second order quantum phase transitions of the *XY* model and shows the influence of finite temperature effects over the zero-temperature critical points. It is shown that the different regions of the $\{T,\lambda\}$ phase diagram of the system above the $T=0$ critical points can be characterized by the different scaling behavior of the metric tensor with temperature. This paper parallels and extends the analysis reported in [21] for the Bures metric. While the quantum Chernoff bound is associated with quantum state discrimination, the Bures metric is related with another natural probabilistic protocol: quantum estimation [22]. Our findings about the quantum Chernoff bound metric show that the same information about the phase diagram of an interacting many-body system can be obtained by using two independent distinguishability measures.

This paper is organized as follows. In Sec. II we introduce the many-body system we analyzed and obtain the corresponding metric tensor in Sec. III. In Sec. IV we carry out the thermal analysis of the metric elements. A global property of the metric is discussed in Sec. V, while conclusions and further research directions are outlined in Sec. VI.

*abasto@usc.edu
†ntj@usc.edu

II. *XY* MODEL

We analyze the quantum phase transitions of the one-dimensional spin chain *XY* model in a transverse magnetic field given by the Hamiltonian

$$H = -\sum_{i=-N-1/2}^{i=N-1/2} \frac{1+\gamma}{2}\sigma_i^x\sigma_{i+1}^x + \frac{1-\gamma}{2}\sigma_i^y\sigma_{i+1}^y + \lambda\sigma_i^z, \quad (1)$$

where the total number of spins N is odd, $\lambda \in \mathbb{R}$ is the transverse magnetic field along the z axis, and $\gamma \in [-1,1]$ is the anisotropy parameter. For $\gamma = \pm 1$ and $\gamma = 0$ we obtain the Ising and *XX* models, respectively. This Hamiltonian can be diagonalized using Jordan-Wigner, Fourier, and Bogoliubov transformations [27]. The diagonalized Hamiltonian is given by $H = \Sigma_{k=-N-1/2}^{k=N-1/2} \Lambda_k \hat{b}_k^\dagger \hat{b}_k$, with Λ_k the quasiparticle energies given by $\Lambda_k = \sqrt{\epsilon_k^2 + \Delta_k^2}$, with $\epsilon_k = \cos(\frac{2\pi k}{N}) - \lambda$ and $\Delta_k = \gamma \sin(\frac{2\pi k}{N})$. One-particle excitations are created by the fermionic operators $\hat{b}_k^\dagger = \cos(\frac{\theta_k}{2})\hat{d}_k^\dagger + i \sin(\frac{\theta_k}{2})\hat{d}_{-k}$ acting on the ground state

$$|\mathrm{gs}(\lambda,\gamma)\rangle = \bigotimes_{k=1}^{N-1/2} \left[\cos\left(\frac{\theta_k}{2}\right)|00\rangle_{k,-k} + i \sin\left(\frac{\theta_k}{2}\right)|11\rangle_{k,-k} \right], \quad (2)$$

with $\hat{d}_k|00\rangle_{k,-k} = \hat{d}_{-k}|00\rangle_{k,-k} = \hat{b}_k|\mathrm{gs}(\lambda,\gamma)\rangle = 0$, and $\cos(\theta_k) = \epsilon_k/\Lambda_k$. This model exhibits a quantum phase transition at two regions in the parameter space $\{\gamma,\lambda\}$: at critical lines $\lambda = \pm 1$, and $\gamma = 0$ for $-1 < \lambda < +1$. At those critical regions the system becomes gapless. In general, the gap Δ is given by $\Delta = |1 - |\lambda||$ if $|\lambda| > |1-\gamma^2|$ (region A); $\Delta = |\gamma|\sqrt{1 - \frac{\lambda^2}{1-\gamma^2}}$ if $|\lambda| < |1-\gamma^2|$ (region B).

III. QUANTUM CHERNOFF BOUND

The quantum Chernoff bound (QCB) is given by

$$\xi_{QCB} = -\ln\left[\min_{0\le s\le 1} \mathrm{Tr}(\rho^s \sigma^{1-s})\right], \quad (3)$$

where $P_{e,\min} = e^{-n\xi_{QCB}}$ is the minimum probability of error in distinguishing two preparations $\rho^{\otimes n}$ and $\sigma^{\otimes n}$ in the limit $n \to \infty$ [24,25]. Defining $Q(\rho,\sigma) = e^{-\xi_{QCB}}$, the quantity $1-Q$ serves as a distinguishability measure between states. Notice that $1 - Q(\rho,\rho) = 0$, and $1 - Q(\rho,\sigma) = 1$ if ρ and σ are orthogonal. Considering two nearby states ρ and $\rho + d\rho$, this quantity induces a metric tensor on the manifold of density operators, with the line element given by

$$ds^2 = \frac{1}{2}\sum_{ij} \frac{|\langle i|d\rho|j\rangle|^2}{(\sqrt{p_i} + \sqrt{p_j})^2}, \quad (4)$$

where $\rho = \Sigma_i p_i |i\rangle\langle i|$ is a spectral decomposition of the density operator. Since we are interested in the finite temperature *XY* model, we consider thermal states of the form $\rho = \frac{e^{-\beta H}}{Z}$. Taking the spectral decomposition of ρ over eigenstates of the Hamiltonian, we can split the metric into two parts so that $ds^2 = ds_c^2 + ds_{nc}^2$, where

$$ds_c^2 = \frac{1}{8}\sum_i \frac{(dp_i)^2}{p_i}, \quad (5)$$

$$ds_{nc}^2 = \frac{1}{2}\sum_{i\neq j} \frac{|\langle i|dj\rangle|^2 (p_i - p_j)^2}{(\sqrt{p_i} + \sqrt{p_j})^2}. \quad (6)$$

We call the first sum the classical part of the metric since it only depends on the Boltzmann weights of the density operator. We label the second sum the nonclassical or quantum part, because it explicitly depends on the states.

In passing we would like to notice that ds_{nc}^2 does not, strictly speaking, define a metric in the parameter space. Indeed one can have curves $t \to \rho(t)$ of density matrices where all the relevant $|j\rangle$ are fixed, e.g., $\rho(t) = \Sigma_i p_i(t)|i\rangle\langle i|$. In other terms, the quadratic form defined at each point of the parameter manifold is just positive semidefinite rather than positive definite and the metric matrix can have zero eigenvalues. This remark has to be kept in mind when one considers the zero-temperature limit $\beta \to \infty$ where, as we will see, $ds \to ds_{nc}$. Moreover, in this limit g_{nc} is nothing but the Fubini-Study metric over the projective state space (the same is obtained by starting from the Bures metric). Once this latter is pulled back to the parameter space null eigenvectors can appear. These vectors correspond to directions along which changing the parameters results in indistinguishable states.

To evaluate the first sum (5), note that

$$\partial_\beta p_i = -(E_i - \langle E\rangle)\frac{e^{-\beta E_i}}{Z},$$

$$\partial_\gamma p_i = -\beta(\partial_\gamma E_i - \langle \partial_\gamma E\rangle)\frac{e^{-\beta E_i}}{Z},$$

$$\partial_\lambda p_i = -\beta(\partial_\lambda E_i - \langle \partial_\lambda E\rangle)\frac{e^{-\beta E_i}}{Z},$$

where $E_i = \Sigma_k n_k \Lambda_k$, $(n_k \in \{0,1\})$.

Summing over states and incorporating the fermion statistics $\langle n_\mu\rangle = (1 + e^{\beta\Lambda_\nu})^{-1}$ and using the free-fermion property $\langle n_\mu n_\nu\rangle - \langle n_\mu\rangle\langle n_\nu\rangle = \delta_{\mu\nu}\langle n_\mu\rangle(1 - \langle n_\mu\rangle)$, we get the following six components for the 3×3 symmetric metric tensor defined by $ds_c^2 = g_{\mu\nu}^c dx^\mu dx^\nu$, $x^\mu \in \{\beta,\gamma,\lambda\}$,

$$g_{\beta\beta}^c = \frac{1}{16}\sum_k \frac{1}{\cosh(\beta\Lambda_k) + 1}\Lambda_k^2, \quad (7)$$

$$g_{\beta\gamma}^c = \frac{\beta}{16\gamma}\sum_k \frac{1}{\cosh(\beta\Lambda_k) + 1}\Delta_k^2, \quad (8)$$

$$g_{\beta\lambda}^c = \frac{-\beta}{16}\sum_k \frac{1}{\cosh(\beta\Lambda_k) + 1}\epsilon_k, \quad (9)$$

$$g_{\gamma\gamma}^c = \frac{\beta^2}{16\gamma^2}\sum_k \frac{1}{\cosh(\beta\Lambda_k + 1)}\frac{\Delta_k^4}{\Lambda_k^2}, \quad (10)$$

$$g_{\gamma\lambda}^c = \frac{-\beta^2}{16\gamma}\sum_k \frac{1}{\cosh(\beta\Lambda_k) + 1}\frac{\epsilon_k\Delta_k^2}{\Lambda_k^2}, \quad (11)$$

$$g^c_{\lambda\lambda} = \frac{\beta^2}{16}\sum_k \frac{1}{\cosh(\beta\Lambda_k)+1}\frac{\epsilon_k^2}{\Lambda_k^2}. \tag{12}$$

In order to find the metric $g^{nc}_{\mu\nu}$ corresponding to ds^2_{nc} we first use the expression for the eigenstates (2) to obtain

$$ds^2_{nc} = \frac{1}{4}\sum_k \frac{\cosh(\beta\Lambda_k)-1}{\cosh(\beta\Lambda_k)+1} d\theta_k^2. \tag{13}$$

Differentiating θ_k along each of our three parameters gives the metric $g^{nc}_{\mu\nu}$. This part of the metric has only three nonzero components, namely,

$$g^{nc}_{\gamma\gamma} = \frac{1}{4\gamma^2}\sum_k \left(\frac{\cosh(\beta\Lambda_k)-1}{\cosh(\beta\Lambda_k)+1}\right)\frac{\epsilon_k^2\Delta_k^2}{\Lambda_k^4}, \tag{14}$$

$$g^{nc}_{\gamma\lambda} = \frac{1}{4\gamma}\sum_k \left(\frac{\cosh(\beta\Lambda_k)-1}{\cosh(\beta\Lambda_k)+1}\right)\frac{\epsilon_k\Delta_k^2}{\Lambda_k^4}, \tag{15}$$

$$g^{nc}_{\lambda\lambda} = \frac{1}{4}\sum_k \left(\frac{\cosh(\beta\Lambda_k)-1}{\cosh(\beta\Lambda_k)+1}\right)\frac{\Delta_k^2}{\Lambda_k^4}. \tag{16}$$

Notice that $g^{nc}_{\lambda\lambda}$ vanishes along the line $\gamma=0$.

IV. THERMAL ANALYSIS OF THE METRIC ELEMENTS

We now proceed to analyze the scaling behavior of the metric elements with temperature, for two characteristic regions in the parameter space $\{\beta,\gamma,\lambda\}$: quantum-critical and quasiclassical. For the quantum-critical case we analyze the scaling at the critical region. For the quasiclassical case we carry out the scaling analysis away from the critical region, for temperatures small enough so that the system looks effectively gapped, i.e., $\beta\Delta \gg 1$. We carry out the analysis in the thermodynamic limit, in which $\frac{2\pi k}{N}\to k$, $\Sigma_k \to \frac{1}{2\pi}\int_{-\pi}^{\pi} dk$ after rescaling $g \to g/N$.

A. Quasiclassical region

We now find the scaling behavior with temperature for the metric element $g^{nc}_{\gamma\gamma}$, in the limit $\beta\Delta \gg 1$. The scaling of all other metric elements can be obtained following procedures similar to those illustrated below.

Since the system is gapped in this region, we have $\beta\Lambda_k > \beta\Delta \gg 1$. This permits us to make the following approximation in the integral expression for $g^{nc}_{\gamma\gamma}$: $\left(\frac{\cosh(\beta\Lambda_k)-1}{\cosh(\beta\Lambda_k)+1}\right) \cong \frac{e^{\beta\Lambda_k}-2}{e^{\beta\Lambda_k}+2} \cong 1-4e^{-\beta\Lambda_k}$. Then, $g^{nc}_{\gamma\gamma}$ can be approximated by

$$g^{nc}_{\gamma\gamma} \cong g^{nc}_{\gamma\gamma}(T=0) - \frac{1}{2\pi}\int_{-\pi}^{\pi} e^{-\beta\Lambda_k}\left(\frac{\epsilon_k \sin(k)}{\Lambda_k}\right)^2.$$

The exponential $e^{-\beta\Lambda_k}$ behaves like a sharp peak in k centered around the absolute minima of Λ_k and can be approximated further by expanding Λ_k to second order in k. The minima of Λ_k occur at $k=0$ for region A, $\lambda>0$; at $k=\pm\arccos\left(\frac{\lambda}{1-\gamma^2}\right)$ for region B; and at $k=\pm\pi$ for region A, $\lambda<0$.

TABLE I. Temperature exponent α, for classical and nonclassical terms of the metric elements in the quasiclassical region. The nonclassical terms follow a behavior given by Eq. (17), while the classical terms behave like Eq. (18).

Region	$g^c_{\beta\beta}$	$g^c_{\beta\lambda}$	$g^c_{\beta\gamma}$	$g^c_{\lambda\lambda}$	$g^c_{\lambda\gamma}$	$g^c_{\gamma\gamma}$	$g^{nc}_{\lambda\lambda}$	$g^{nc}_{\lambda\gamma}$	$g^{nc}_{\gamma\gamma}$
A	1/2	−1/2	1/2	−3/2	−1/2	1/2	3/2	3/2	3/2
B	1/2	−1/2	−1/2	−3/2	−3/2	−3/2	1/2	1/2	1/2

Due to the peak of $e^{-\beta\Lambda_k}$, the rest of the integrand can be approximated by its value at the minimum of Λ_k in region B, or expanded until second order in k in region A. Taking the limits of integration to be from $-\infty$ to ∞, this approximation results in Gaussian integrals, with the result given by

$$g^{nc}_{\gamma\gamma}(\beta\Delta \gg 1) = g^{nc}_{\gamma\gamma}(T=0) - f(\lambda,\gamma)T^\alpha e^{-\Delta/T}, \tag{17}$$

where the exponent α of the temperature is equal to 3/2 for region A, and 1/2 for region B. Each metric element will have a different $f(\lambda,\gamma)$. Similarly, the classical terms of the metric elements can be approximated by

$$g^c(\beta\Delta \gg 1) = h(\lambda,\gamma)T^\alpha e^{-\Delta/T}. \tag{18}$$

In Table I we summarize the scaling in temperature for all the metric elements in the quasiclassical region.

B. Quantum-critical region

Consider now taking $T\to 0$ at the values of γ and λ for which $\Delta=0$. Since in this limit $\beta\to\infty$, all classical metric elements vanish due to the factor of $[\cosh(\beta\Lambda_k)+1]^{-1}$ in front. We are left only to analyze the nonclassical part of the metric, namely, $g^{nc}_{\gamma\gamma}$, $g^{nc}_{\gamma\lambda}$, and $g^{nc}_{\lambda\lambda}$. There are three cases to consider: (i) $\gamma=0$ and $\lambda=\pm 1$, (ii) $\gamma=0$ and $-1<\lambda<1$, and (iii) $\gamma\neq 0$ and $\lambda=\pm 1$. Since $g^{nc}_{\gamma\lambda}$ and $g^{nc}_{\lambda\lambda}$ are multiplied by an overall factor of γ, both vanish for cases (i) and (ii).

The dispersion Λ_k is an even function of k, so we can restrict ourselves to the interval $k\in[0,\pi]$. For cases (ii) and (iii) Λ_k is linear in k about its root, whereas for the case (i) Λ_k is quadratic about its root.

We now show how to calculate the scaling in temperature of the metric element $g^{nc}_{\gamma\gamma}$ for case (i). A similar procedure applies to $g^{nc}_{\lambda\lambda}$ and $g^{nc}_{\gamma\lambda}$ for the other cases. The goal is to bound the metric element above and below by functions that have the same scaling behavior in β. This will ensure that the metric itself must scale with the same exponent.

Since the dispersion Λ_k is quadratic around the root $k=0$, we can approximate it as $\Lambda_k \sim \frac{k^2}{2}$. Define the piecewise function

$$f(\beta,k) = \begin{cases} \dfrac{\beta^2 k^4}{16} & \text{for } 0 \le k \le \dfrac{2}{\sqrt{\beta}} \\ 1 & \text{for } \dfrac{2}{\sqrt{\beta}} \le k \le \pi \end{cases}, \tag{19}$$

which for all β and k satisfies

TABLE II. Scaling behavior with temperature at criticality, for the metric elements $g^{nc}_{\lambda\lambda}$, $g^{nc}_{\gamma\lambda}$, and $g^{nc}_{\gamma\gamma}$. Note that $g^{nc}_{\lambda\lambda}$ and $g^{nc}_{\gamma\lambda}$ are exactly 0 for $\gamma=0$.

	$\lambda=\pm1,\gamma=0$	$\lambda=\pm1,\gamma\neq0$	$\lambda\in(-1,1),\gamma=0$
$g^{nc}_{\lambda\lambda}$	0	T^{-1}	0
$g^{nc}_{\gamma\lambda}$	0	const$+O(T)$	0
$g^{nc}_{\gamma\gamma}$	$T^{-1/2}$	const$+O(T^3)$	T^{-1}

$$\frac{f(\beta,k)}{2} < \frac{\cosh\left(\frac{\beta k^2}{2}\right)-1}{\cosh\left(\frac{\beta k^2}{2}\right)+1} < f(\beta,k). \tag{20}$$

We can now split the integral into two parts.

$$g^{nc}_{\gamma\gamma} = \frac{1}{4\pi}\int_0^{\pi} dk \frac{\cosh(\beta\Lambda_k)-1}{\cosh(\beta\Lambda_k)+1}\frac{\epsilon_k^2\sin^2(k)}{\Lambda_k^4}$$

$$\simeq \frac{1}{4\pi}\int_0^{2/\sqrt{\beta}} dk \frac{\cosh\left(\frac{\beta k^2}{2}\right)-1}{\cosh\left(\frac{\beta k^2}{2}\right)+1}\frac{4}{k^2} \tag{21}$$

$$+\frac{1}{4\pi}\int_{2/\beta}^{\pi} dk \frac{\cosh(\beta\Lambda_k)-1}{\cosh(\beta\Lambda_k)+1}\frac{\epsilon_k^2\sin^2 k}{\Lambda_k^4}, \tag{22}$$

where we have taken $\Lambda_k \sim \frac{k^2}{2}$ and $\sin(k)\sim k$ for the integral (21). Note that this is a good approximation for $\beta\to\infty$, since the upper integration limit becomes arbitrarily close to 0.

We can now bound the first integral above and below, using the function (19),

$$\frac{1}{4\pi}\int_0^{2/\sqrt{\beta}} dk \frac{f(\beta,k)}{2}\frac{4}{k^2} \le \frac{1}{4\pi}\int_0^{2/\sqrt{\beta}} dk \frac{\cosh\left(\frac{\beta k^2}{2}\right)-1}{\cosh\left(\frac{\beta k^2}{2}\right)+1}\frac{4}{k^2}$$

$$\le \frac{1}{4\pi}\int_0^{2/\sqrt{\beta}} dk f(\beta,k)\frac{4}{k^2}..$$

These bounding integrals scale as $\beta^{1/2}$. Therefore the first integral (21) must also scale as $\beta^{1/2}$ for $\beta\to\infty$.

Over the entire interval $[0,\pi]$ we can bound Λ_k^{-1} from above by $\frac{6}{k^2}$, upper bound $\sin^2(k)$ by k^2, and replace the ratio of hyperbolic cosines in Eq. (22) by $f(\beta,k)$. This will bound integral (22) from above, as

$$\frac{1}{4\pi}\int_{2/\sqrt{\beta}}^{\pi} dk \frac{\cosh(\beta\Lambda_k)-1}{\cosh(\beta\Lambda_k)+1}\frac{\epsilon_k^2\sin^2 k}{\Lambda_k^4} \le \frac{1}{4\pi}\int_{2/\sqrt{\beta}}^{\pi} dk \frac{36}{k^2} \sim \beta^{1/2}.$$

Therefore, since the second integral (22) scales as a power of $\frac{1}{2}$ or lower in β, $g^{nc}_{\gamma\gamma}$ must scale as $\beta^{1/2}$ to highest order. Table II lists the scaling for all three nonclassical metric elements.

The behavior of the nonclassical metric elements in the quantum-critical region can be inferred from dimensional scaling analysis as was done in [21], for zero temperature. Though carried out for the Bures metric, it applies also for the quantum Chernoff bound metric. From [21] we see that the scaling dimension of the nonclassical metric elements $g^{nc}_{\lambda\lambda}$, $g^{nc}_{\gamma\lambda}$, and $g^{nc}_{\gamma\gamma}$ is given by $\Delta_{nc}=\Delta_\mu+\Delta_\nu-2z-d$, where Δ_μ,Δ_ν are the scaling dimensions of the operators that couple to $\mu,\nu\in\{\lambda,\gamma\}$ and produce the quantum phase transitions, z is the dynamical exponent, and d is the spatial dimensionality. The finite temperature in the quantum system transforms into a finite additional length dimension in the classical system so that

$$g^{nc} \sim T^{\Delta_{nc}/z}. \tag{23}$$

The findings summarized in Table II are consistent with this relation, assuming that $\Delta_\gamma=2,\Delta_\lambda\geq3$ (first column, $z=2$); $\Delta_\gamma=3,\Delta_\lambda=1$ (second column, $z=1$); $\Delta_\gamma=1,\Delta_\lambda\geq2$ (third column, $z=1$). The condition $\Delta_x<d+z$ ($d=1$) signals the relevance, in the renormalization group sense [23], of the operator weighted by the coupling constant x ($x=\gamma,\lambda$).

Intuitively, shifting some parameter toward a critical value should result in a significant change in the state of our system. That is, the direction in parameter space corresponding to maximal distinguishability should be toward or away from the critical regions. Indeed we see that the diverging metric element in the gapless quantum critical case corresponds exactly to this direction of maximal distinguishability. As an example, for $\lambda=\pm1$ and $\gamma\neq0$ only $g_{\lambda\lambda}$ diverges. Changing λ and keeping γ constant here corresponds to the direction of maximal distinguishability, which is along the $g_{\lambda\lambda}$ contribution to the line element. In the Ising model limit, where $\gamma=1$, our results for the metric scaling agree exactly with that of [21], where the Bures metric was used.

V. MAXIMUM EIGENVALUE

In this brief section we consider the maximum eigenvalue of the metric g for each point in parameter space. Since g is a symmetric matrix, this corresponds to the matrix norm $\|g\|=\max_{\|\mathbf{v}\|=1}|\langle\mathbf{v},g\mathbf{v}\rangle|$. The associated eigenvectors define the field of maximum distinguishability directions. An analogous analysis for the Bures metric has been presented in [21]. From the inequalities $\max_{i,j}|g_{ij}|\leq\|g\|\leq9\max_{i,j}|g_{ij}|$ one immediately sees that the maximal eigenvalue of g diverges if and only if at least one of the matrix elements of g diverges. In other words, $\|g\|$ encodes global information about the metric that one can extract without analyzing each of the matrix elements separately.

Shown in Fig. 1 is a contour plot of the maximum eigenvalues of g. The critical regions are clearly revealed as those values of the parameters for which some metric elements diverge for small temperature.

VI. CONCLUSION

In this paper we have employed the metric tensor induced on the parameter space by the quantum Chernoff bound to study the finite-temperature phase diagram of the anisotropic

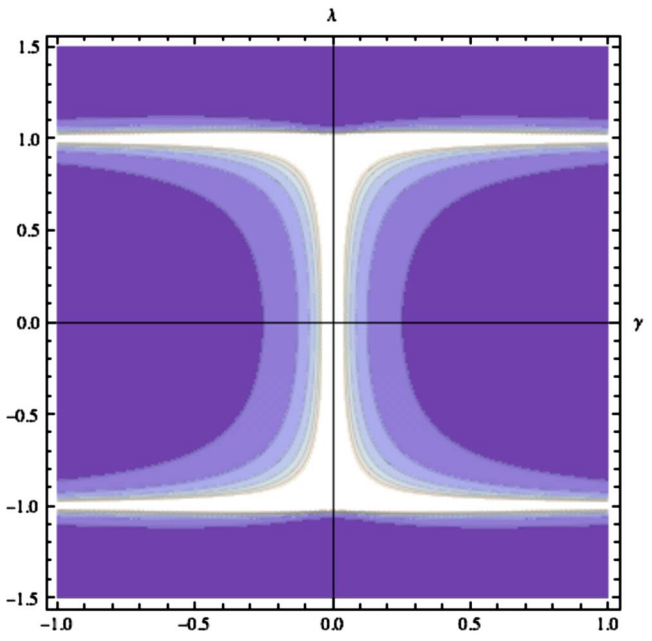

FIG. 1. (Color online). Contour plot of the maximum eigenvalue of g for $-1.5<\lambda<1.5$, $-1<\gamma<1$, and $T=10^{-2}$. The color scale goes from 0 (purple) to 3 (white). The critical regions can be clearly identified.

XY spin chain. We have shown that the temperature scaling of the metric elements has a different form in the quasiclassical and quantum-critical cases. In the quasiclassical case, where the temperature T is much smaller than the energy gap Δ, the metric elements vanish exponentially in $1/T$; in the quantum-critical regime $\Delta/T\ll 1, T\to 0$, the behavior is a power law in T. Moreover, in the quasiclassical case the specific behavior in temperature depends on the functional form of the gap Δ, and in the quantum-critical case the nonclassical metric element, which diverges in the limit of $T\to 0$, is the one corresponding to the relevant parameter driving the QPT. We would like to notice that, in view of the operational meaning of the quantum Chernoff bound metric in quantum state discrimination tasks, these results suggest that quantum criticality may provide a resource for quantum state discrimination protocols. This connection has been elaborated in [22] for the related quantum estimation problem. Another problem that is worthy of investigation and has not been touched in this paper is the role of the curvature tensor associated to the metric g. The preliminary findings for the same quantity in the pure state case [10] and in the Bures metric case [21] suggest that the curvature might provide additional information about the nature of the critical lines and location of crossover regions.

The analysis reported in this paper for the *XY* chain is quite close in spirit and technicalities to the one for the Bures metric in the quantum Ising model case [21]. In both cases the important physical features of the low-temperature phase diagram of the systems, e.g., quantum-critical to quasiclassical crossovers, can be identified by resorting to a metric with a statistical distinguishability meaning. This proves that the information-theoretic metrical approach to quantum criticality [10] is not bound to the use of a special single metric. Different choices of distinguishability measure may provide essentially the same physical information.

ACKNOWLEDGMENTS

We would like to thank M. Cozzini, P. Giorda, and L. Campos Venuti for fruitful discussions. D.F.A. and N.T.J. are grateful to the Quantum Unit of the ISI Foundation for its hospitality and for providing a stimulating scientific environment.

[1] S. Sachdev, *Quantum Phase Transitions* (Cambridge University Press, Cambridge, England, 1999); M. Vojta, Rep. Prog. Phys. **66**, 2069 (2003).
[2] A. Osterloh, L. Amico, G. Falci, and R. Fazio, Nature (London) **416**, 608 (2002).
[3] T. J. Osborne and M. A. Nielsen, Phys. Rev. A **66**, 032110 (2002); Quantum Inf. Process. **1**, 45 (2002).
[4] G. Vidal, J. I. Latorre, E. Rico, and A. Kitaev, Phys. Rev. Lett. **90**, 227902 (2003).
[5] L.-A. Wu, M. S. Sarandy, and D. A. Lidar, Phys. Rev. Lett. **93**, 250404 (2004).
[6] T. R. de Oliveira, G. Rigolin, M. C. de Oliveira, and E. Miranda, Phys. Rev. Lett. **97**, 170401 (2006).
[7] L. Amico, R. Fazio, A. Osterloh, and J. V. Vedral, e-print arXiv:quant-ph/0703044, Rev. Mod. Phys. (to be published).
[8] P. Zanardi and N. Paunkovic, Phys. Rev. E **74**, 031123 (2006).
[9] Y. Chen, P. Zanardi, Z. D. Wang, and F. C. Zhang, New J. Phys. **8**, 97 (2006).
[10] P. Zanardi, P. Giorda, and M. Cozzini, Phys. Rev. Lett. **99**, 100603 (2007).
[11] L. Campos Venuti and P. Zanardi, Phys. Rev. Lett. **99**, 095701 (2007).
[12] P. Zanardi, M. Cozzini, and P. Giorda, J. Stat. Mech.: Theory Exp. (2007), L02002.
[13] M. Cozzini, P. Giorda, and P. Zanardi, Phys. Rev. B **75**, 014439 (2007).
[14] M. Cozzini, R. Ionicioiu, and P. Zanardi, Phys. Rev. B **76**, 104420 (2007).
[15] P. Zanardi, H.-T. Quan, X.-G. Wang, and C.-P. Sun, Phys. Rev. A **75**, 032109 (2007).
[16] P. Buonsante and A. Vezzani, Phys. Rev. Lett. **98**, 110601 (2007).
[17] M.-F. Yang, Phys. Rev. B **76**, 180403(R) (2007); H.-Q. Zhou and J. P. Barjaktarevic, e-print arXiv:cond-mat/0701608.
[18] H.-Q. Zhou, J.-H. Zhao, and B. Li, e-print arXiv:0704.2940; H.-Q. Zhou, e-print arXiv:0704.2945.
[19] Y.-C. Tzeng and M.-F. Yang, Phys. Rev. A **77**, 012311 (2008).
[20] L. Campos Venuti and P. Zanardi, Phys. Rev. Lett. **99**, 095701 (2007).
[21] P. Zanardi, L. Campos Venuti, and P. Giorda, Phys. Rev. A **76**,

062318 (2007).
[22] P. Zanardi and M. G. A. Paris, e-print arXiv:0708.1089.
[23] N. Goldenfeld, *Lectures on Phase Transitions and the Renormalization Group* (Westview Press, Boulder, 1992).
[24] K. M. R. Audenaert, J. Calsamiglia, R. Munoz-Tapia, E. Bagan, L. Masanes, A. Acin, and F. Verstraete, Phys. Rev. Lett. **98**, 160501 (2007).
[25] M. Nussbaum and A. Szkoła, e-print arXiv:quant-ph/0607216.
[26] H. Chernoff, Ann. Math. Stat. **23**, 493 (1952).
[27] J. I. Latorre, E. Rico, and G. Vidal, Quantum Inf. Comput. **4**, 48 (2004).